Scanning Electron Microscopy Analysis of the Adaptation of Single-Unit Screw-Retained Computer-Aided Design/Computer-Aided Manufacture Abutments After Mechanical Cycling

Roberto Adrian Markarian, DDS, MS, PhD[1]/Deborah Pedroso Galles, DVM, MS[2]/
Fabiana Mantovani Gomes França, DS, MS, PhD[3]

Purpose: *To measure the microgap between dental implants and custom abutments fabricated using different computer-aided design/computer-aided manufacture (CAD/CAM) methods before and after mechanical cycling.* ***Materials and Methods:*** *CAD software (Dental System, 3Shape) was used to design a custom abutment for a single-unit, screw-retained crown compatible with a 4.1-mm external hexagon dental implant. The resulting stereolithography file was sent for manufacturing using four CAD/CAM methods (n = 40): milling and sintering of zirconium dioxide (ZO group), cobalt-chromium (Co-Cr) sintered via selective laser melting (SLM group), fully sintered machined Co-Cr alloy (MM group), and machined and sintered agglutinated Co-Cr alloy powder (AM group). Prefabricated titanium abutments (TI group) were used as controls. Each abutment was placed on a dental implant measuring 4.1 × 11 mm (SA411, SIN) inserted into an aluminum block. Measurements were taken using scanning electron microscopy (SEM) (×4,000) on four regions of the implant-abutment interface (IAI) and at a relative distance of 90 degrees from each other. The specimens were mechanically aged (1 million cycles, 2 Hz, 100 N, 37°C) and the IAI width was measured again using the same approach. Data were analyzed using two-way analysis of variance, followed by the Tukey test.* ***Results:*** *After mechanical cycling, the best adaptation results were obtained from the TI (2.29 ± 1.13 µm), AM (3.58 ± 1.80 µm), and MM (1.89 ± 0.98 µm) groups. A significantly worse adaptation outcome was observed for the SLM (18.40 ± 20.78 µm) and ZO (10.42 ± 0.80 µm) groups. Mechanical cycling had a marked effect only on the AM specimens, which significantly increased the microgap at the IAI.* ***Conclusion:*** *Custom abutments fabricated using fully sintered machined Co-Cr alloy and machined and sintered agglutinated Co-Cr alloy powder demonstrated the best adaptation results at the IAI, similar to those obtained with commercial prefabricated titanium abutments after mechanical cycling. The adaptation of custom abutments made by means of SLM or milling and sintering of zirconium dioxide were worse both before and after mechanical cycling.* Int J Oral Maxillofac Implants 2017 (10 pages). doi: 10.11607/jomi.5588

Keywords: *CAD/CAM, dental implant, external abutment connection, implant-abutment interface, microgap, misfit*

The efficiency of computer-aided design/computer-aided manufacture (CAD/CAM) restorations and the cost eff ctiveness of CAD/CAM systems have driven the increased use of such technologies.[1] The main techniques used to create CAD/CAM restorations are based on additive or subtractive manufacturing, the latter being more common. Subtractive strategies involve computer-assisted sculpting of restorative material blocks with drills or diamond burs until they reach the desired shape; additive strategies involve three-dimensional (3D) sculpting of the object with deposition of successive layers.[2,3] Diff rent materials are available for the manufacturing of components and prostheses via CAD/CAM technology.

Zirconium dioxide is indicated for implant-supported CAD/CAM restorations and is prepared via subtractive milling to produce abutments for cemented restorations, structural copings for direct esthetic layering, and mesostructures.[4–8] Zirconia offers good esthetics, biocompatibility, shade stability, low accumulation of plaque, good resistance to abrasion, and low thermal conductivity[9]; however, when high mechanical resistance

[1]Private Practice, São Paulo, Brazil.
[2]Private Practice, São Paulo, Brazil.
[3]Professor. São Leopoldo Mandic Institute and Dental Research Center, Campinas/São Paulo, Brazil.

Correspondence to: Dr Roberto Adrian Markarian, R. Martiniano de Carvalho 864 cj 105, 01321-000, São Paulo-SP, Brazil. Email: roberto@implart.com.br

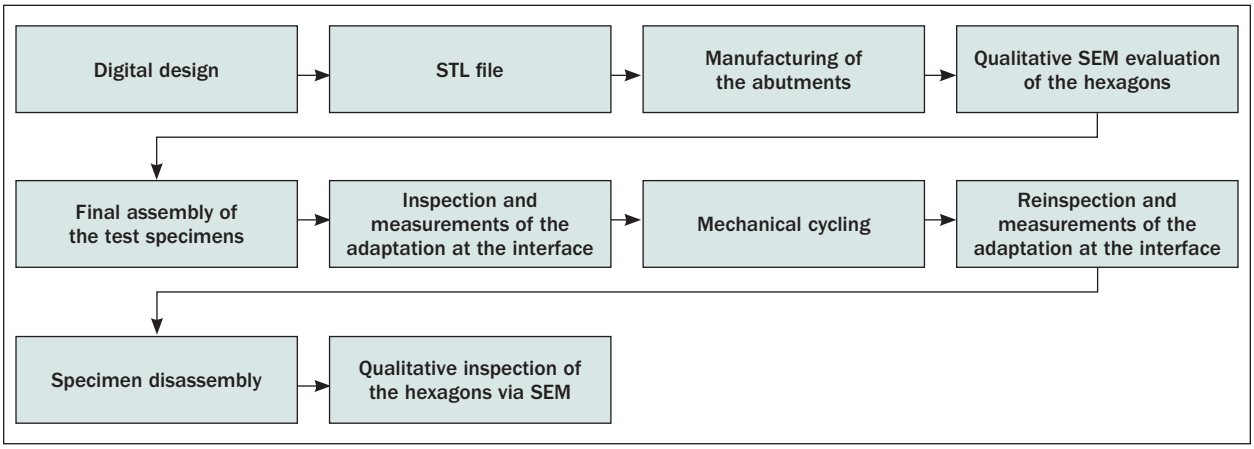

Fig 1 Study flowchart. STL = stereolithography.

is required, clinicians prefer metal-alloy structures such as titanium or precious metals.[10,13]

Cobalt-chromium (Co-Cr) alloys are used in prosthetic structures because of their favorable mechanical and chemical properties, ease of use, and cost effectiveness when compared with precious metal alloys.[14] Co-Cr is frequently used in laboratory casting processes; however, recent developments have enabled the use of such alloys with CAD/CAM technologies via subtractive strategies, milling machines,[15] or additive approaches.[16,17]

Only a few industrial computer numeric control (CNC) milling machines or especially large CAD/CAM milling machines for dental laboratories are able to produce structures from fully sintered blocks of Co-Cr on a large scale because of the hardness of the material.[18] To widen access to this technology, a Co-Cr alloy for CAD/CAM has been developed (Ceramill Sintron) and presented in the form of metal blocks composed of pressed powder and binding polymers to increase stability.[19] The manufacturing method using agglutinated Co-Cr allows machining of dry material with subtractive techniques using less robust equipment.[18] The processing steps involved in Co-Cr alloy preparation are comparable to those of zirconia because the material needs to be machined into relatively high dimensions then immediately sintered in a special furnace in the presence of argon to achieve its chemical and mechanical properties, which are comparable to those of cast Co-Cr alloys.[18,20–22]

The additive strategy of selective laser melting (SLM), also known as laser sintering, uses fine granules of metals such as titanium and Co-Cr as raw material, which are fused by a laser beam guided by 3D coordinates obtained from a computerized prototype. After successive vertical layers of material are sintered, the structure reaches its final volumetric dimensions.[16,23,24] The SLM technique can produce more complex 3D specimens than those produced by means of subtractive techniques.[2] The SLM and sintered metal milling technologies have been studied for the development of prosthetic structures over natural teeth,[17,25] as well as abutments for single-tooth implants.[26]

Only a few long-term follow-up in vivo studies of implant-supported single-unit CAD/CAM abutments have been published.[4,27] Clinically, customized single-unit abutments prepared via CAD/CAM milling in titanium or zirconia for implants in the anterior region have shown good performance and have been associated with superior soft tissue stability when compared with prefabricated abutments.[28,29] Therefore, it is important to simulate aging in vitro by applying external forces and estimating clinical behavior, which can be achieved by means of mechanical cycling.[30–34]

Dental CAD/CAM systems allow the implant-abutment interface (IAI) to be created by two strategies: *(1)* cementing the customized abutment onto a prefabricated titanium-based abutment, or *(2)* directly designing the customized abutment, including the IAI. The first method is usually indicated by implant manufacturers, whereas the second method can be used in some clinical settings.[5,7]

The use of prefabricated titanium-based abutments is recommended to ensure that the IAI fit is optimal, as parts are produced according to the original manufacturer's specific tions, resulting in high mechanical stiffness and failure load.[7] However, a customized CAD/CAM abutment, including the IAI, can be manufactured with any material and strategy used in desktop laboratory machines. Within these approaches, concern may arise regarding the precision achieved at the IAI level and the resistance of the abutments resulting from these methods.[5,7,8,26]

During function, masticatory forces generate stress not only in the abutment but also in the implant and supporting tissues, which can be exacerbated should the IAI be ill fittin ,[35] resulting in bacterial leakage and peri-implant colonization.[36] Scanning electron microscopy (SEM) has been proven successful not only at measuring the IAI adaptation,[37–39] but also at revealing wear spots on both abutments and implants.[30]

 doi: 10.11607/jomi.5588

Table 1 Descriptions of Experimental Groups, Materials, and Composition (n = 10 each)

Group	Manufacturing method	Equipment	Material specifications
TI	CNC prefabricated	SIN	Titanium abutment (AI 4151-Q)
ZO	CNC milling machine	Roders, RXD5	Zirconium dioxide (Zcad, Metoxit)
SLM	Selective laser melting	EOSINT M270, EOS	Cobalt-chromium in power (EOS Cobalt Chrome SP2; EOS)
MM	CNC milling machine	Neoshape, Neodent	Fully sintered cobalt-chromium (Neodent Milling Center)
AM	Desktop milling machine	Ceramill Motion II, Amann Girrbach	Agglutinated cobalt-chromium (Ceramill Sintron, Amann Girrbach)

The objective of this study was to evaluate, by SEM, the IAI adaptation of customized single-unit CAD/CAM abutments manufactured via four methods and subjected to mechanical cycling while observing the effects of mechanical cycling on the abutments. The null hypothesis was that mechanical cycling and the type of material used to fabricate CAD/CAM abutments do not interfere with implant/abutment adaptation.

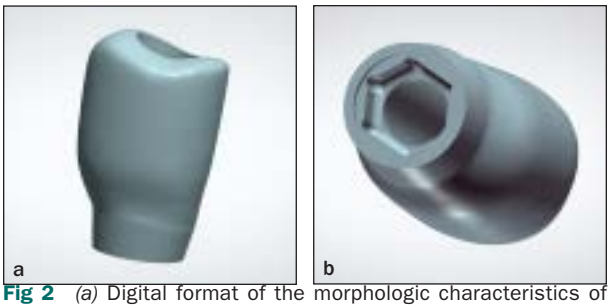

Fig 2 *(a)* Digital format of the morphologic characteristics of the customized abutment designed for this study. *(b)* Characteristics of the interface of the customized abutment.

MATERIALS AND METHODS

Abutments

A fl wchart of the experimental stages is shown in Fig 1. The samples were prepared as single-unit abutments with a 4.1-mm–diameter external hexagon and antirotation platform. A 4.1-mm external hex implant analog (AN 4100, SIN) was scanned (D700, 3Shape A/S) and used as the prototype connection. Using drawing software (Dental System, 3Shape A/S), a digital custom abutment measuring 4.1 × 9.6 mm was designed for a single-unit screwed-on restoration in the premolar region. The abutment was meant to engage the implant hexagon and would require further porcelain application (Fig 2). The resulting stereolithography (STL) file format was used to manufacture abutments according to four methods, and 10 identical abutments were made for each group (Table 1). Titanium cylinders with antirotation hexagon (AI 4151-Q, SIN) were used as control abutments (TI group). Once the abutments were obtained from the manufacturer, they were cleaned in an ultrasonic bath containing 96% ethanol for 5 minutes. The groups were as follows:

- ZO group: A CNC milling machine (Roders, RXD5) was used. Zirconia milling was performed in a presintered stage with dimensions increased by 25%. This step was followed by sintering of the structures in a furnace (In Fire, Sirona), which caused the structure to shrink.
- SLM group: The project was sent to a machining center (CUBO) that used an SLM machine (EOSINT M270, EOS) and a Co-Cr alloy powder (EOS Cobalt Chrome SP2, EOS) as raw material. A diamond disc was then used to separate the samples from their base.
- MM group: For preparation of the Co-Cr specimens, the STL file as sent to a CNC machining center (Neoshape). The abutments were carved directly from a block of dense and completely sintered Co-Cr alloy, which needed no further treatment.
- AM group: The specimens were prepared on laboratory-based machining equipment (Ceramill Motion II, Amann Girrbach). The alloy was machined into a bonded phase (Ceramill Sintron, Amann Girrbach) with dimensions increased by 10%. The abutments were then sintered in a furnace (Ceramill ArgoTherm) in the presence of argon gas at 1,300°C, according to the manufacturer's instructions. The abutment samples obtained using CAD/CAM methods are shown in Fig 3.

Test Specimens Setup

For the final assembly of the specimens, external hexagon titanium implants (n = 50) measuring 4 mm in diameter and 11 mm in length with a 4.1-mm platform (SA411, SIN) were used. Using an implant insertion key (CCIT 20, SIN) and a manual ratchet (TMECC, SIN), the authors inserted the implants individually into 50 aluminum blocks measuring 7 × 7 × 11 mm and featuring a 3.5-mm diameter and an 8-mm-deep central orifi e.

To comply with the International Organization for Standardization (ISO) 14801 standard (dentistry fatigue test for endosseous dental implants), 3 mm of the implants were left exposed to simulate vertical bone loss. Using a square-headed retaining screw (PTQ 2008, SIN) and manual torque of 32 Ncm, the authors then

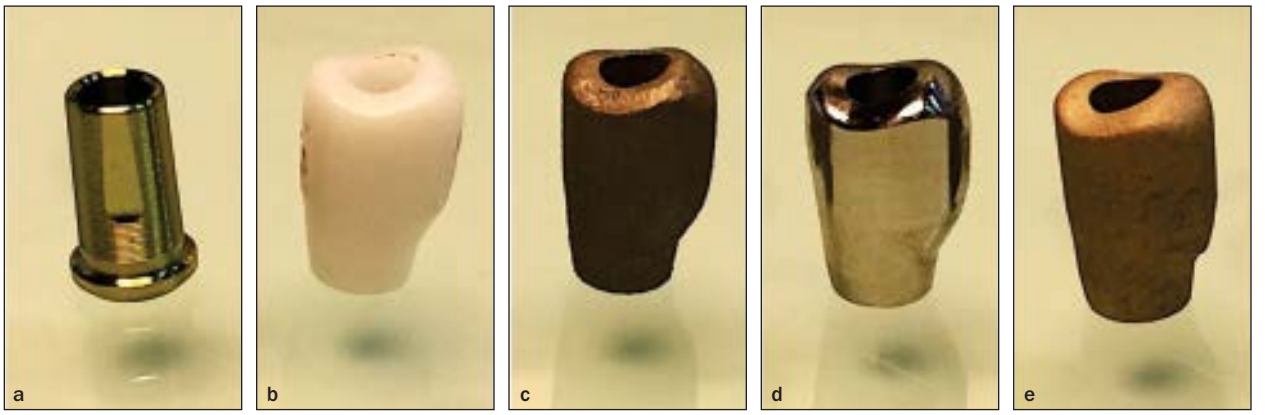

Fig 3 Samples of the components obtained using CAD/CAM methods. *(a)* Prefabricated titanium (TI). *(b)* Zirconia (ZO). *(c)* Selective laser melting (SLM). *(d)* Machined metal (MM). *(e)* Agglutinated metal (AM).

Fig 4 Test specimen after implant placement into aluminum blocks and abutment adaptation.

fi ed each abutment onto the implant with a dedicated key (CQTM20, SIN), a manual ratchet (TMEC, SIN), and a digital torque wrench (TQ-8800, Lutron) (Fig 4).

Mechanical Cycling

To simulate masticatory forces, the implant-abutment sets were subjected to 1 million mechanical fatigue cycles (Byocycle, Biopdi) at a frequency of 2 Hz under 100 N and 30-degree angulation. The specimens were kept in saline solution at 37°C throughout the experiment.

SEM Analysis of Abutment Fit

SEM (×4,000 magnific tion) was used to take adaptation measurements at the IAI before and after mechanical cycling. Four markings were made on each specimen with relative distances of 90 degrees so that vertical misfit measurements could be taken corresponding to the distance between the bottom edge of each abutment and the top edge of the implant. The same calibrated observer took all measurements. The average of the four measurements (µm) for each specimen was used as the reference value for each sample.

SEM Analysis of the Abutment Hexagon Surfaces

For the evaluation of marginal adaptation, all abutments were observed by means of SEM at ×50 magnific tion (Quanta FEG 250, FEI) at the fitting face of the hexagon before and after mechanical cycling. One of the edges was then chosen at random to be inspected at ×250 magnific tion.

Statistical Analysis

The assumptions of normality and homoscedasticity for the adaptation values between implants and abutments were evaluated with Shapiro-Wilk and Levene tests, respectively. Repeated-measures two-way analysis of variance (ANOVA) was applied to determine whether the mismatch between implants and abutments was influen ed by abutment type and mechanical cycling. The Tukey test was used for the breakdown of interactions. Statistical calculations were performed with SPSS 20 at a significan e level of 5%.

RESULTS

Quantitative Evaluation of the IAI

The Shapiro-Wilk and Levene tests indicated that the data did not conform to a normal distribution ($P < .05$) and they did not show homoscedasticity ($P < .001$). A normal distribution was achieved, however, by applying a logarithmic transformation of the data ($P > .05$). The repeated-measures two-way ANOVA applied to the transformed data revealed a significa t interaction between abutment type and mechanical cycling ($P > .001$, 83.8% test power).

Before mechanical cycling, lower adaptation values were found for the TI and AM groups, which were not significa tly different from each other (Table 2). The worst adaptation values were found in the ZO and SLM

 doi: 10.11607/jomi.5588

Table 2 Mean (Standard Deviation) Adaptation Values (μm) Between Implants and Abutments Before and After Mechanical Cycling

Abutment type	Before mechanical cycling	After mechanical cycling
TI (control)	1.103 (0.306)^{Aa}	2.296 (1.136)^{Aa}
ZO	11.746 (0.605)^{Ca}	10.428 (0.806)^{Ba}
SLM	24.705 (15.293)^{Ca}	18.405 (20.789)^{Ba}
MM	2.609 (1.133)^{Ba}	1.898 (0.987)^{Aa}
AM	1.098 (0.724)^{Aa}	3.583 (1.801)^{Ab}

Uppercase and lowercase letters represent comparison of the data with Tukey test. Means followed by different uppercase letters indicate a significant difference between abutment types with respect to the conditions before and after mechanical cycling. Means followed by different lowercase letters indicate a significant effect of mechanical cycling, with each type of abutment considered separately.

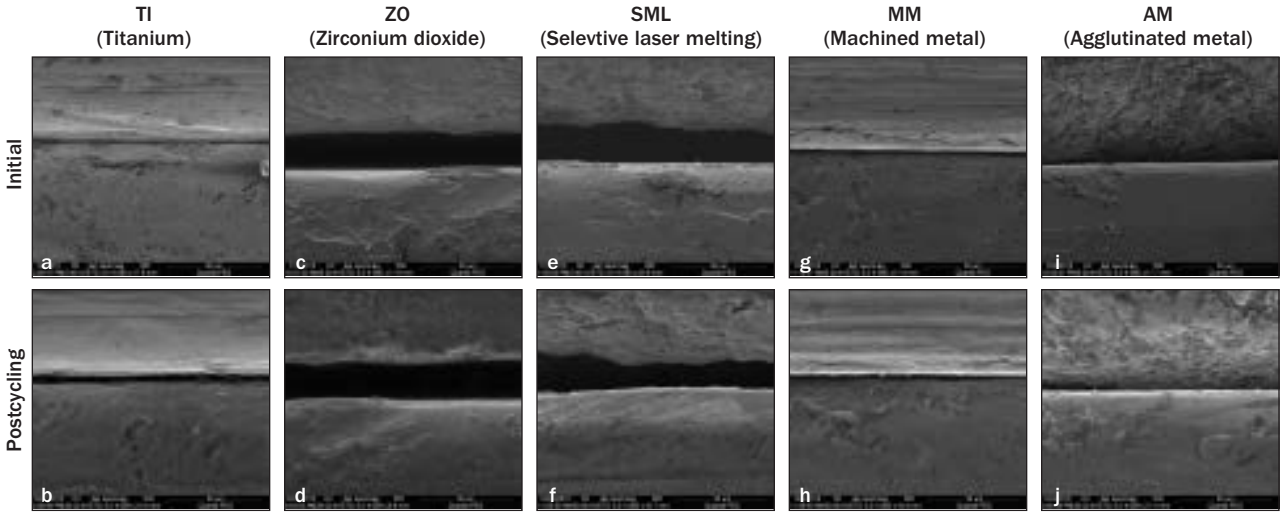

Fig 5 Examples of interfaces before and after mechanical cycling of the different materials tested. *(a)* TI group before cycling. *(b)* TI group after cycling. *(c)* ZO group before cycling. *(d)* ZO group after cycling. *(e)* SLM group before cycling. *(f)* SLM group after cycling. *(g)* MM group before cycling. *(h)* MM group after cycling. *(i)* AM group before cycling. *(j)* AM group after cycling.

groups, which also were not significa tly different from each other. The adaptation values obtained from the MM group showed intermediate values, which were significa tly different from those found for the other abutment types.

On completion of mechanical cycling, the Tukey test indicated lower adaptation values for the abutments in the MM, TI, and AM groups, with no significa t differences between them. The ZO and SLM groups exhibited the highest misfit values, which were not significa tly different from each other. Mechanical cycling had a significa t effect on adaptation values only for the AM group, leading to a significa t increase in misfi .

Qualitative Evaluation via SEM

The lateral walls of the TI group abutments appeared fl ttened and contained some grooves (Fig 5a) according to SEM inspection of adaptation at the IAI and hexagons. These specimens had regular and well-defined edges that were not affected by mechanical cycling (Figs 5b, 6c, and 6d).

At ×4,000 magnific tion, evidence of mild roughness and unevenness was observed on the lateral walls of the abutments in the ZO group, with loss of definition of the abutment edges (Fig 5c). After mechanical cycling, the abutment edges did not change; however, a smear layer could be seen on the hexagonal surface of the interface (Figs 5d and 7d).

The specimens in the SLM group exhibited moderate surface roughness, as well as irregularities on the walls and edges (Figs 5e and 5f). Inspection of the interface revealed deformation of the abutment edges and the presence of lumps and beads of material. Qualitative changes were not observed after mechanical cycling (Figs 8c and 8d).

The lateral surfaces of the abutments in the MM group were flattened and contained slight grooves and dimples inherent to the machining process, which was similar to the TI group (Fig 5g). The specimens had regular and well-defined edges and did not appear to have been affected by mechanical cycling (Figs 5h and Fig 9d). At the hex connection interface, some artifacts

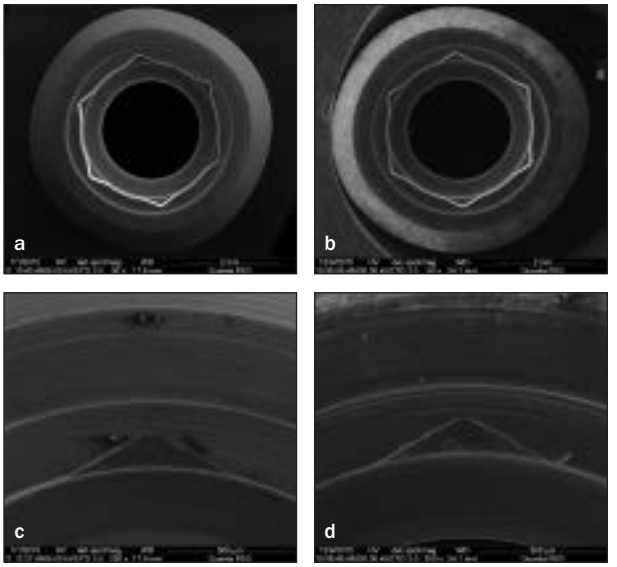

Fig 6 Qualitative analysis of an abutment from the control group (TI) before and after mechanical cycling. *(a)* Hexagon before mechanical cycling (×50 magnification). *(b)* Hexagon after mechanical cycling (×50). *(c)* Hexagon before mechanical cycling (×250). *(d)* Hexagon after mechanical cycling (×250).

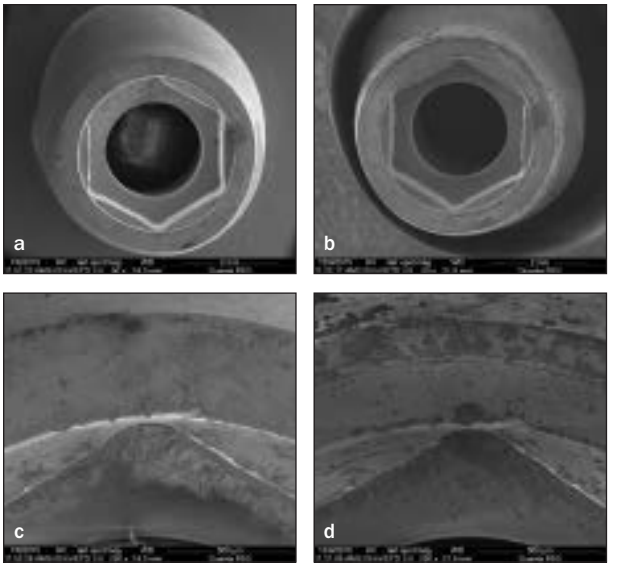

Fig 7 Qualitative analysis of an abutment from the ZO group before and after mechanical cycling. *(a)* Hexagon before mechanical cycling (×50 magnification). *(b)* Hexagon after mechanical cycling (×50). *(c)* Hexagon before mechanical cycling (×250). *(d)* Hexagon after mechanical cycling (×250).

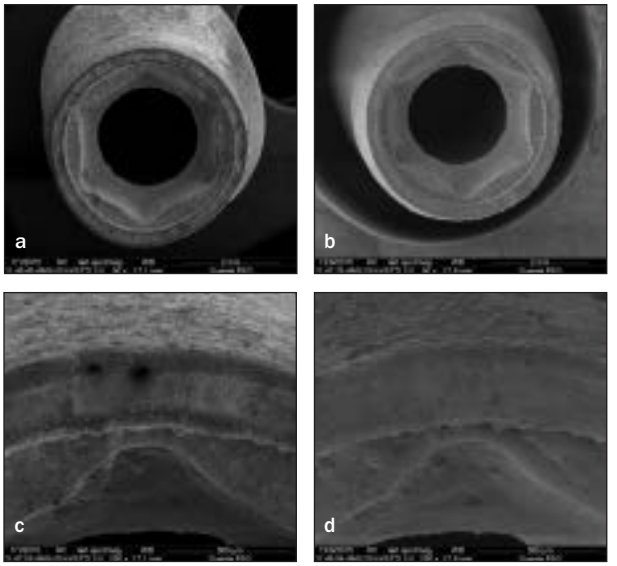

Fig 8 Qualitative analysis of an abutment from the SLM group before and after mechanical cycling. *(a)* Hexagon before mechanical cycling (×50 magnification). *(b)* Hexagon after mechanical cycling (×50). *(c)* Hexagon before mechanical cycling (×250). *(d)* Hexagon after mechanical cycling (×250).

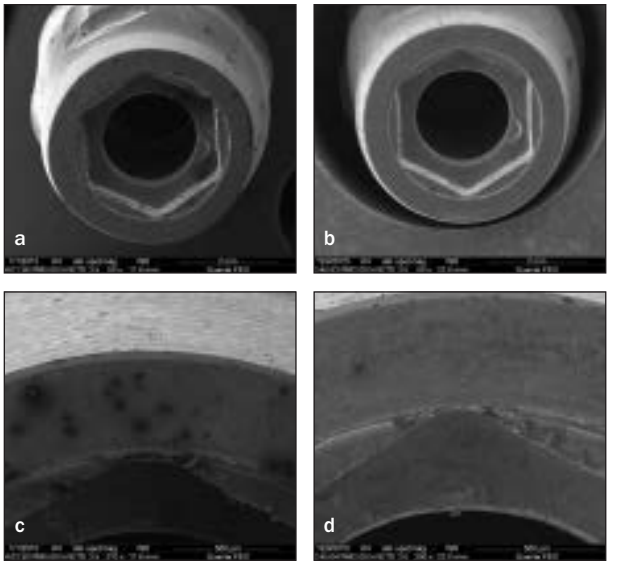

Fig 9 Qualitative analysis of an abutment from MM group before and after mechanical cycling. *(a)* Hexagon before mechanical cycling (×50 magnification). *(b)* Hexagon after mechanical cycling (×50). *(c)* Hexagon before mechanical cycling (×250). *(d)* Hexagon after mechanical cycling (×250).

were observed such as chips and beads of material (Figs 9a and 9c). After mechanical cycling, these beads disappeared, leaving a smear layer on the interface surface (Fig 9d).

The abutments in the AM group exhibited markedly rough lateral surfaces with rounded edges (Fig 5i). Inspection of the interface revealed microtexture patterns and loss of definition of the dihedral angles despite the smooth appearance of the abutment and the absence of artifacts macroscopically. The characteristics of the interface did not change after mechanical cycling (Figs 5j and 10d).

DISCUSSION

CAD/CAM permits abutment designs of customized dimensions using a variety of materials.[1] CAD/CAM abutments are designed to produce a highly accurate IAI; however, some manufacturing factors—including the use of additive or subtractive strategies, the quality of the milling machine, and the intrinsic properties of the preparation material—may interfere with high-standard adaptation.[3]

The manufacturing process influen ed the adaptation of single-unit CAD/CAM abutments in this study, and the null hypothesis was therefore rejected. The abutments in the TI group were machined by the same manufacturer as that of the implants. This process followed strict specific tions for maximum precision of the implant-abutment set, obtaining average values of 1 µm. Similar mean values were obtained for the abutments in the AM group, which, under inspection by SEM, were free of internal irregularities and debris (Fig 10c). Intermediate adaptation values of about 2.5 µm were obtained for abutments in the MM group, which were prepared on a CNC machine and exhibited artifacts such as beads and debris at the interface that may have interfered with the quality of the initial adaptation (Fig 9c). The abutments from the SLM and ZO groups had the highest misfit values (> 10 µm). In the case of the ZO abutments, no evidence of changes were observed at the interface according to SEM (Fig 7c); however, for the SLM abutments, a marked morphologic change in roughness throughout the abutment surface at the interface region (Fig 8c) was observed when compared with the control group (TI) (Fig 6b).

Solá-Ruíz et al[39] investigated the baseline adaptation of external hexagon titanium abutments by interchanging components between different commercial systems and classified the adaptation level as acceptable, good, or excellent, with values typically below 10 µm and average values below 4 µm. Results below 10 µm were also found in the literature for fi ed prostheses prepared by CAD/CAM in zirconia,[12] titanium, and Co-Cr.[11] In the present study, after mechanical loading, the abutments in the TI, MM, and AM groups showed similar adaptation values, and all were within the same range as those reported in the literature for external hexagon implant abutments.[37,39] Metal abutments made by CAD/CAM systems using subtractive milling techniques appear to be highly accurate. Moreover, although the abutments in the ZO and SLM groups exhibited a decrease in average misfi , this finding was not significa t and remained at high levels, possibly because the causal factors of the initial misfit ere maintained.

Fernández et al[26] investigated the adaptation of single-unit CAD/CAM abutments for external hexagon implants fabricated in Co-Cr using SLM and milling techniques and compared them with cast abutments.

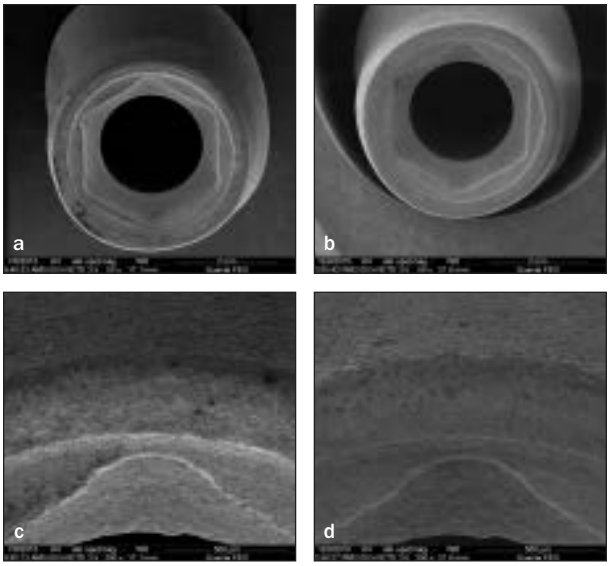

Fig 10 Qualitative analysis of an abutment from AM group before and after mechanical cycling. *(a)* Hexagon before mechanical cycling (×50 magnification). *(b)* Hexagon after mechanical cycling (×50). *(c)* Hexagon before mechanical cycling (×250). *(d)* Hexagon after mechanical cycling (×250).

They reported average adaptation values in the respective order of 11.3 µm, 0.73 µm, and 9.09 µm. They found that the abutments prepared by means of SLM exhibited high superficial roughness and loss of definition of the edges, with a positive correlation between internal roughness and abutment adaptation.[26]

The above results are consistent with those found in this study using SEM, which demonstrated considerable roughness on the abutments in the SLM group. The roughness did not change after mechanical cycling, which is similar to the results for agglutinated metal powder abutments (AM). Clinically, this roughness could translate into greater bacterial colonization on the unpolished inner surfaces of the abutment and enhance bacterial count at the IAI (Figs 8c and 10c). The relevance of such bacterial accumulation must be investigated thoroughly because contamination at the IAI always occurs to some extent.[37] Jansen et al[36] studied microbial infilt ation on 13 implant-abutment configu ations and reported that a good marginal seal of implant components can reduce bacterial leakage, though no system was able to prevent it altogether.

The lateral surfaces of the abutments in the MM group contained some grooves and undulations similar to those in the TI group (Fig 5g). The interface showed well-defined geometry and angles (Fig 9a). The artifacts initially found at the IAI of the MM abutments were probably secondary to overheating during milling, considering the high wear resistance of the material.[3,14]

The friction between the components during mechanical cycling probably created the smear layer and the small chippings seen on the surface of the components. The same friction could have caused the beads of material to disappear (Fig 9d).

The titanium abutments in the control group exhibited well-defined margins and some grooves on the walls from the CNC tools (Fig 5a); these abutments did not appear to have undergone any qualitative changes after mechanical cycling (Fig 5b). The good results for these abutments may encourage the use of titanium-based abutments in CAD/CAM systems. Some manufacturers propose digital systems for which titanium-based abutments are used and onto which a monolithic crown[7] or a mesostructure[4,5] can be designed, in theory ensuring the best possible fi between the implant and the prosthetic system and less susceptibility to aging by mechanical fatigue. The use of titanium-based abutments, however, introduces questions about their mechanical stability, the strength of the cement layer between the interface and the mesostructure, and bacterial colonization of the cementation zone.[5] According to the results of this study, these intermediate structures could also be adequately designed with good adaptation outcomes using techniques and materials from the MM and AM groups.

Mechanical cycling methods vary widely in the literature in number of masticatory cycles, force applied, specimen angulation, and frequency.[33] In general, studies seem to report no change in adaptation levels of single-unit abutments after mechanical cycling, as observed for single-unit cast abutments[31] and abutments prepared by means of CAD/CAM alumina, zirconia, and titanium.[6] Moreover, Cibirka et al[32] observed macroscopic changes on implant and abutment hexagons after 5 million cycles, despite no change in countertorque or loosening of the screws.

In this study, the simulation of 15 months of clinical use was performed on the abutments,[34] which did not affect the level of marginal fit in any of the groups except for AM, thus causing the null hypothesis to be rejected. Agglutinated Co-Cr is a novel material, about which only a few in vitro[18–20] and no clinical studies have been performed. It is unclear if the presence of organic agglutinating substances influen es their ultimate strength or the degree of porosity resulting from sintering. One possible reason for such findings could be the sintering process, which can cause dimensional changes.[21] In addition, the images from the interfaces suggest a certain degree of horizontal misalignment of the components from this group (Fig 5j), which was not investigated further in this study.

The ZO group abutments exhibited a regular and well-defined macroscopic shape on SEM at ×250 magnific - tion (Fig 7a); however, irregularities could be detected at ×4,000 (Fig 5c). After mechanical cycling, no further damage to the abutments was detected (Figs 5d and 7b), though smear deposits were observed at the hexagonal interface of all zirconia abutments, probably caused by friction between components (Fig 7d). This finding corroborates those of a study by Stimmelmayr et al,[30] who reported debris, irregularities, and increased wear on the implant interface connected to zirconia abutments compared with titanium abutments after mechanical cycling.

Custom ceramic abutments prepared by CAD/CAM systems provide good results because of their structural stability.[9] Linkevicius and Vaitelis[10] found that single-unit titanium and zirconia abutments performed well clinically, with zirconia having the esthetic advantage. The authors stated that titanium should be the material of choice because of its stability over time, but other materials may be used for restorations involving direct application of porcelain to zirconia and Co-Cr. The results of the present study are consistent with these finding , as the best qualitative and quantitative adaptation results were achieved with titanium abutments.

Some studies have found that CAD/CAM-fabricated single-unit abutments made of zirconia performed just as well as prefabricated titanium abutments,[6,12,13] whereas others reported worse performance.[8] In the present study, the adaptation values of abutments in the ZO group were significa tly poorer than those of abutments in the TI group. This difference might be related to certain stages of the manufacturing process and to intrinsic properties of the material.[3] The abutments in the TI group were processed on a large CNC milling machine, and no comparisons were made with other machines on the market. Zirconium dioxide is machined at an increased volume, which requires use of a special heating furnace at a high temperature to achieve the fina sintering. Therefore, the sintering stage could distort the marginal adaptation of zirconia abutments secondary to abutment shrinkage.[15]

Milling and direct metal laser sintering using SLM strategies are preferable to conventional casting techniques.[25] Theoretically, the low ductility of casting Co-Cr would not allow for finely detailed structures and, therefore, milling would be more suitable to reproducing details.[20] On the other hand, criticism of milling techniques includes equipment vibrations and the use of drills that may become worn and unable to reproduce all required detail in prosthetic structures.[2,17]

Hypothetically, marginal adaptation of abutments prepared by means of SLM would be equal to or slightly better than metal casting and certainly better than milling.[25] However, in this study, the laser-sintered material exhibited high internal distortion and sharp marginal surface roughness, as well as irregularities of the walls and edges that generated the most significa t misfi observed in this study. Also, the specimens in the SLM

 doi: 10.11607/jomi.5588

group exhibited higher fit measurements, as well as a low consistency with respect to the manufacturing process (as evidenced by a higher standard deviation), which would hinder its clinical application for prosthetic structures over implants.

No significa t additional changes to the abutments occurred after mechanical cycling. One possible explanation for the distortions observed in the SLM group could be the intensity of the laser. Takaichi et al[24] found that different laser intensities can generate completely different microstructures; therefore, an investigation of the optimal energy level could be conducted to maximize the accuracy of implant structures. In addition, the SLM process generates residual stresses within the material because of rapid heating and cooling of the alloy, which may affect the accuracy of the final structure.[23] For this reason, an additional heating step should be included so that this residual stress can be released, which also can alter the microstructure of the alloy.[24]

The vertical misfit of the components may not be the only type of distortion in custom abutments prepared by means of CAD/CAM because it is a 3D displacement and, as such, can be classified as vertical, horizontal, angular, and rotational.[33] The vertical misfit should be as low as possible to prevent overloading of the components and supporting tissues.[35] The quality of the internal adaptation to the abutment-implant system and the horizontal mismatch should also be investigated further, which can be achieved using cross sections or longitudinal sections of the specimens.[37,39]

It can be inferred that titanium remains the gold standard for single-unit implant abutments, but machined Co-Cr or agglutinated Co-Cr may be an alternative in select cases, especially when ceramics should be applied directly onto the coping surface. The SLM technique should be studied further before intensive clinical use is initiated for implants.

CONCLUSIONS

This research aimed to measure the microgap between external-connection dental implants and CAD/CAM abutments made of different materials—milled zirconia, Co-Cr alloy sintered via SLM, machined and fully sintered Co-Cr alloy, and machined agglutinated Co-Cr alloy powder—when compared with prefabricated Ti abutments before and after mechanical cycling.

On the basis of these finding , and considering the limitations of this study, the following conclusions can be drawn:

1. Custom CAD/CAM abutments in the MM and AM groups demonstrated adaptation levels similar to those of prefabricated titanium abutments (control group) after mechanical cycling.
2. The adaptation levels of CAD/CAM abutments in the SLM and ZO groups remained at the highest levels among the tested groups before and after mechanical cycling.
3. Mechanical cycling significa tly increased the misfit alues of agglutinated Co-Cr abutments (AM groups), which remained at the lowest levels among the tested groups. Mechanical cycling had no effect on the other types of abutments.

ACKNOWLEDGMENTS

The authors acknowledge the dental laboratory EsteticArt, São Paulo, Brazil, for digital abutment design. They also thank SIN, São Paulo, for its support by donating the implants and prosthetic components, and CEME/UNIFESP, São Paulo, for the SEM analyses. The authors declare no conflicts of interest with regard to any entity related to the products mentioned in this article.

REFERENCES

1. Joda T, Brägger U. Digital vs conventional implant prosthetic workflows: A cost/time analysis. Clin Oral Implants Res 2015;26:1430–1435.
2. van Noort R. The future of dental devices is digital. Dent Mater 2012;28:3–12.
3. Abduo J, Lyons K, Bennamoun M. Trends in computer-aided manufacturing in prosthodontics: A review of the available streams. Int J Dent 2014;2014:783948.
4. Zembic A, Bösch A, Jung RE, Hämmerle CH, Sailer I. Five-year results of a randomized controlled clinical trial comparing zirconia and titanium abutments supporting single-implant crowns in canine and posterior regions. Clin Oral Implants Res 2013;24:384–390.
5. Mühlemann S, Truninger TC, Stawarczyk B, Hämmerle CH, Sailer I. Bending moments of zirconia and titanium implant abutments supporting all-ceramic crowns after aging. Clin Oral Implants Res 2014;25:74–81.
6. Yüzügüllü B, Avci M. The implant-abutment interface of alumina and zirconia abutments. Clin Implant Dent Relat Res 2008;10:113–121.
7. Joda T, Bürki A, Bethge S, Brägger U, Zysset P. Stiffness, strength, and failure modes of implant-supported monolithic lithium disilicate crowns: Influence of titanium and zirconia abutments. Int J Oral Maxillofac Implants 2015;30:1272–1279.
8. Baldassarri M, Hjerppe J, Romeo D, Fickl S, Thompson VP, Stappert CF. Marginal accuracy of three implant-ceramic abutment configurations. Int J Oral Maxillofac Implants 2012;27:537–543.
9. Volpato CÂM, D'Altoé Garbelotto LG, Fredel MC, Bondioli F. Application of zirconia in dentistry: Biological, mechanical and optical considerations. In: Sikalidis C (ed). Advances in Ceramics—Electric and Magnetic Ceramics, Bioceramics, Ceramics and Environment. Rijeka, Croatia: InTech Open Access Publisher, 2011. https://www.intechopen.com/books/advances-in-ceramics-electric-and-magnetic-ceramics-bioceramics-ceramics-and-environment/application-of-zirconia-in-dentistry-biological-mechanical-and-optical-considerations. Accessed 27 April 2017.
10. Linkevicius T, Vaitelis J. The effect of zirconia or titanium as abutment material on soft peri-implant tissues: A systematic review and meta-analysis. Clin Oral Implants Res 2015;26(suppl):s139–s147.
11. Svanborg P, Stenport V, Eliasson A. Fit of cobalt–chromium implant frameworks before and after ceramic veneering in comparison with CNC-milled titanium frameworks. J Clin Exp Dent 2015;1:49–56.
12. Abduo J, Lyons K, Waddell N, Bennani V, Swain M. A comparison of fit of CNC-milled titanium and zirconia frameworks to implants. Clin Implant Dent Relat Res 2012;14(suppl):e20–e29.

13. Vigolo P, Fonzi F, Majzoub Z, Cordioli G. An in vitro evaluation of titanium, zirconia, and alumina procera abutments with hexagonal connection. Int J Oral Maxillofac Implants 2006;21575–21580.
14. Al Jabbari YS. Physico-mechanical properties and prosthodontic applications of Co-Cr dental alloys: A review of the literature. J Adv Prosthodont 2014;6:138–145.
15. de França DG, Morais MH, das Neves FD, Barbosa GA. Influence of CAD/CAM on the fit accuracy of implant-supported zirconia and cobalt-chromium fixed dental prostheses. J Prosthet Dent 2015;113:22–28.
16. Koutsoukis T, Zinelis S, Eliades G, Al-Wazzan K, Rifaiy MA, Al Jabbari YS. Selective laser melting technique of Co-Cr dental alloys: A review of structure and properties and comparative analysis with other available techniques. J Prosthodont 2015;24:303–312.
17. Tuna SH, Özçiçek Pekmez N, Kürkçüoğlu I. Corrosion resistance assessment of Co-Cr alloy frameworks fabricated by CAD/CAM milling, laser sintering, and casting methods. J Prosthet Dent 2015;114:725–734.
18. Stawarczyk B, Eichberger M, Hoffmann R, et al. A novel CAD/CAM base metal compared to conventional CoCrMo alloys: An in-vitro study of the long-term metal-ceramic bond strength. Oral Health Dent Manag 2014;13:446–452.
19. Li KC, Prior DJ, Waddell JN, Swain MV. Comparison of the microstructure and phase stability of as-cast, CAD/CAM and powder metallurgy manufactured Co–Cr dental alloys. Dent Mater 2015;31:e306–e315.
20. Lee DH, Lee BJ, Kim SH, Lee KB. Shear bond strength of porcelain to a new millable alloy and a conventional castable alloy. J Prosthet Dent 2015;113:329–335.
21. Becker BS, Bolton JD, Youseffi . Production of porous sintered co-cr-mo alloys for possible surgical implant applications: Part 1: Compaction, sintering behaviour, and properties. Int J Powder Metall 1995;38:201–208.
22. Dourandish M, Godlinski D, Simchi A, Firouzdor V. Sintering of biocompatible P/M Co-Cr-Mo alloy (F-75) for fabrication of porosity-graded composite structures. Mater Sci Eng A Struct Mater 2008;472:338–346.
23. Lu Y, Wu S, Gan Y, et al. Investigation on the microstructure, mechanical property and corrosion behavior of the selective laser melted CoCrW alloy for dental application. Mater Sci Eng C Mater Biol Appl 2015;49:517–525.
24. Takaichi A, Suyalatu, Nakamoto T, et al. Microstructures and mechanical properties of Co-29Cr-6Mo alloy fabricated by selective laser melting process for dental applications. J Mech Behav Biomed Mater 2013;21:67–76.
25. Oyagüe RC, Sánchez-Turrión A, López-Lozano JF, Suárez-García MJ. Vertical discrepancy and microleakage of laser-sintered and vacuum-cast implant-supported structures luted with different cement types. J Dent 2012;40:123–130.
26. Fernández M, Delgado L, Molmeneu M, García D, Rodríguez D. Analysis of the misfit of dental implant-supported prostheses made with three manufacturing processes. J Prosthet Dent 2014;111:116–123.
27. Patzelt SB, Spies BC, Kohal RJ. CAD/CAM-fabricated implant-supported restorations: A systematic review. Clin Oral Implants Res 2015;26(suppl):s77–s85.
28. Lops D, Bressan E, Parpaiola A, Sbricoli L, Cecchinato D, Romeo E. Soft tissues stability of cad-cam and stock abutments in anterior regions: 2-year prospective multicentric cohort study. Clin Oral Implants Res 2015;26:1436–1442.
29. Borges T, Lima T, Carvalho A, Dourado C, Carvalho V. The influence of customized abutments and custom metal abutments on the presence of the interproximal papilla at implants inserted in single-unit gaps: A 1-year prospective clinical study. Clin Oral Implants Res 2014;25:1222–1227.
30. Stimmelmayr M, Edelhoff , Güth JF, Erdelt K, Happe A, Beuer F. Wear at the titanium-titanium and the titanium-zirconia implant-abutment interface: A comparative in vitro study. Dent Mater 2012;28:1215–1220.
31. Hecker DM, Eckert SE, Choi YG. Cyclic loading of implant-supported prostheses: Comparison of gaps at the prosthetic-abutment interface when cycled abutments are replaced with as-manufactured abutments. J Prosthet Dent 2006;95:26–32.
32. Cibirka RM, Nelson SK, Lang BR, Rueggeberg FA. Examination of the implant-abutment interface after fatigue testing. J Prosthet Dent 2001;85:268–275.
33. Assunção WG, dos Santos PH, Delben JA, Gomes ÉA, Barao V, Tabata LF. Effect of misfit on preload maintenance of retention screws of implant-supported prostheses. J Mater Eng Perform 2008;18:935–938.
34. Dittmer MP, Dittmer S, Borchers L, Kohorst P, Stiesch M. Influence of the interface design on the yield force of the implant–abutment complex before and after cyclic mechanical loading. J Prosthodont Res 2012;56:19–24.
35. Markarian RA, Ueda C, Sendyk CL, Laganá DC, Souza RM. Stress distribution after installation of fixed frameworks with marginal gaps over angled and parallel implants: A photoelastic analysis. J Prosthodont 2007;16:117–122.
36. Jansen VK, Conrads G, Richter EJ. Microbial leakage and marginal fit of the implant-abutment interface. Int J Oral Maxillofac Implants 1997;12:527–540.
37. Dias EC, Bisognin ED, Harari ND, et al. Evaluation of implant-abutment microgap and bacterial leakage in five external-hex implant systems: An in vitro study. Int J Oral Maxillofac Implants 2012;27:346–351.
38. Coelho AL, Suzuki M, Dibart S, Da Silva N, Coelho PG. Cross-sectional analysis of the implant–abutment interface. J Oral Rehabil 2007;34:508–516.
39. Solá-Ruíz MF, Selva-Otaolaurruchi E, Senent-Vicente G, González-de-Cossio I, Amigó-Borrás V. Accuracy combining different brands of implants and abutments. Med Oral Patol Oral Cir Bucal 2013;18:e332–e336.